A Laser Fluorosensor for Maritime Surveillance: Measurement of Oil Spills

R. Reuter, H. Wang[1], R. Willkomm and K. Loquay

Carl von Ossietzky University of Oldenburg, Physics Department,
D-26111 Oldenburg, Germany

T. Hengstermann and A. Braun

Optimare GmbH, D-26386 Wilhelmshaven

ABSTRACT

In 1991 a Dornier DO228-212 aircraft was put into operation by the German Ministry of Transport for maritime surveillance of the German responsibility areas in the North Sea and the Baltic Sea. The aircraft is equipped with a Side-Looking Airborne Radar and a UV/IR scanner for the detection of oil spills. To achieve a higher performance, a new Microwave Radiometer developed at DLR Oberpfaffenhofen and a Laser Fluorosensor were integrated in 1993. This paper describes the design and specifications of the Laser Fluorosensor. This is the first instrument of its kind which meets the operational requirements for long-term use on board of an aircraft. By using a conical scanner, it allows two-dimensional mapping of the sea surface in the nadir range, with 150 m swath width from 300 m aircraft altitude. The method of interpreting fluorescence data in terms of substance types by using the principal component analysis of fluorescence spectra is discussed. Data obtained in an airborne performance test are presented. Several oil spills were analyzed in this experiment, and the results are displayed as maps of oil film thickness and substance classes on the sea surface.

INTRODUCTION

In 1985 two Dornier DO 28 D2 aircraft were procured for maritime surveillance by the Federal Ministry of Transport and by the Coastal Federal States of Bremen, Hamburg, Lower Saxony and Sleswig-Holstein. Operated by the Naval Air Wing 5 in Kiel, these aircraft were equipped with side-looking airborne radar (SLAR) for detecting oil slicks over large distances, a UV/IR scanner for mapping the sea surface in the nadir-range, and TV and photocameras (Schroh and Bustorff, 1989).

Based on experience with this equipment, and as a result of the development of new sensors at research institutes, the Ministry of Transport decided in 1988 to develop a new maritime surveillance system. In addition to the approved sensors utilized up to that time in the first generation aircraft, the new system would include also a microwave radiometer (MWR) and a laser fluorosensor (LFS). The two sensors were under development at DLR Oberpfaffenhofen and at the University of Oldenburg with support from the Federal Ministry of Research and Technology. The rationale of using these instruments is that they allow a wider analysis of oil spills in terms of film thickness, and hence discharged volume. LFS data contain also information on the type of spilled substance. Moreover, some hydrographic and biological data can be measured, such as seawater turbidity and concentrations of phytoplankton and gelbstoff which are useful parameters for estimating ecological conditions in coastal waters. Another new component of the system is a central operator console (COC) for the control of instruments, data display and storage. A Dornier DO 228-212 aircraft allows for a flight time of up to 6 hours during operations at sea. An overview of this second generation surveillance system in an early stage of its realization is given by Grüner et al. (1991).

The hydrographic fluorescence lidar is described extensively in the literature, see, for example, the review by Measures (1984). For a detailed description of the methods of oil film thickness measurements and oil type evaluation with fluorescence lidar we refer to articles published by O'Neil et al. (1980), Hoge and Swift (1980, 1983), Burlamacchi et al. (1983), Hengstermann and Reuter (1990, 1992c), Dudelzak et al. (1991), Verdebout and Koechler (1992), and to other publications cited by these authors. Signals from natural organic compounds of seawater, like gelbstoff and phytoplankton pigments, interfere in general with the fluorescence emission of oils, and need consider-

[1] Now with Physikaliench-Technische Bundesanstalt, D-38116 Braunschweig, Germany.

ation when interpreting the data. The measurement of these naturally occurring substances is described in Poole and Esaias (1982), Exton et al. (1983), Bristow et al (1985), Hoge et al. (1986a,b), Reuter et al. (1993), and in other papers cited there.

Layout and specifications of the LFS developed at the University of Oldenburg have been described in detail elsewhere (Grüner et al., 1991; Hengstermann et al., 1992a), and are only briefly summarized here. The purpose of this paper is to report on the results of an airborne experiment performed in 1992 with this instrument. This experiment was an acceptance test for a future routine application of the LFS as a component of the maritime surveillance aircraft of the Ministry of Transport in the German responsibility areas of the North Sea and the Baltic Sea. For the first time, a two-dimensional imagery of the film thickness distribution of oil slicks was achieved in this experiment with an airborne laser fluorosensor, including also a mapping of the oil classification.

1. THE LASER FLUOROSENSOR

The LFS (Fig. 1) is an airborne fluorescence lidar for analyzing the upper layers of the sea from aircraft flight altitudes of 100 to 300 m. It consists of

- a XeCl excimer laser for the analysis of oils and other organic pollutants, and of gelbstoff,
- an excimer laser-pumped dye laser with an emission wavelength suitable for chlorophyll fluorescence excitation, and hence for the measurement of phytoplankton distributions,
- a Schmidt-Cassegrainian telescope with 20 cm entrance aperture, and a 12 channel spectrograph realized with dichroic beamsplitters, interference filters and compact PMT (Fig. 2),

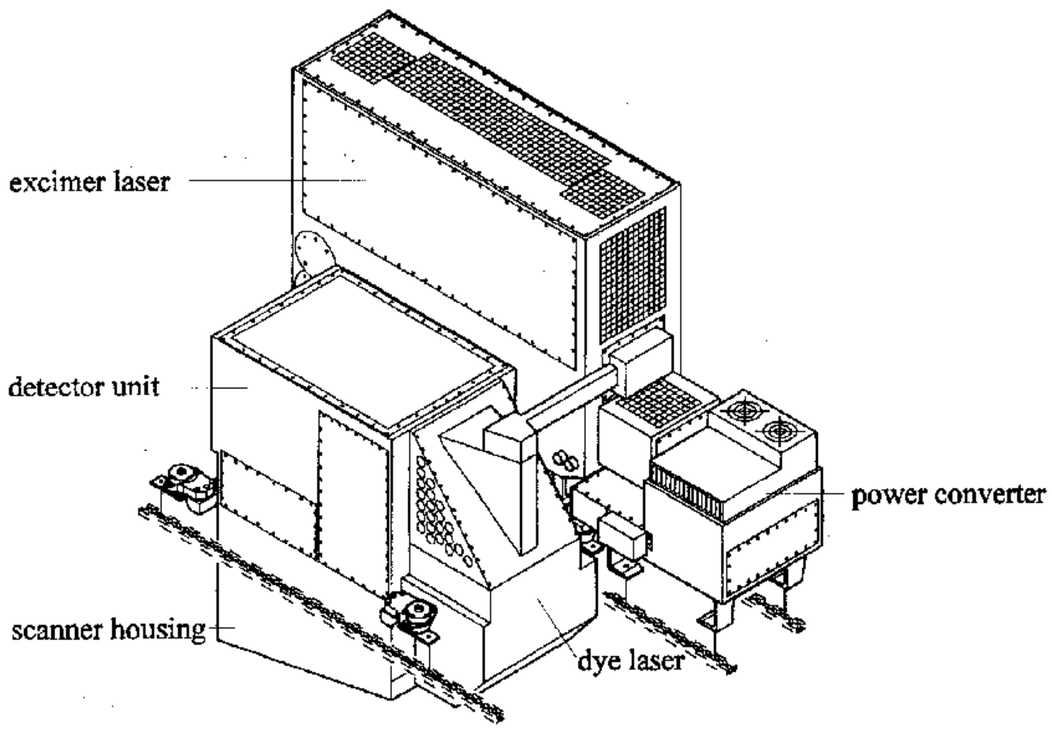

Fig. 1 - Scheme of the laser fluorosensor and the integration into the aircraft. Position is above a bottom hatch which is closed on its lower side by a 60 cm diameter quartz window for protection of optical components against dust and humidity.

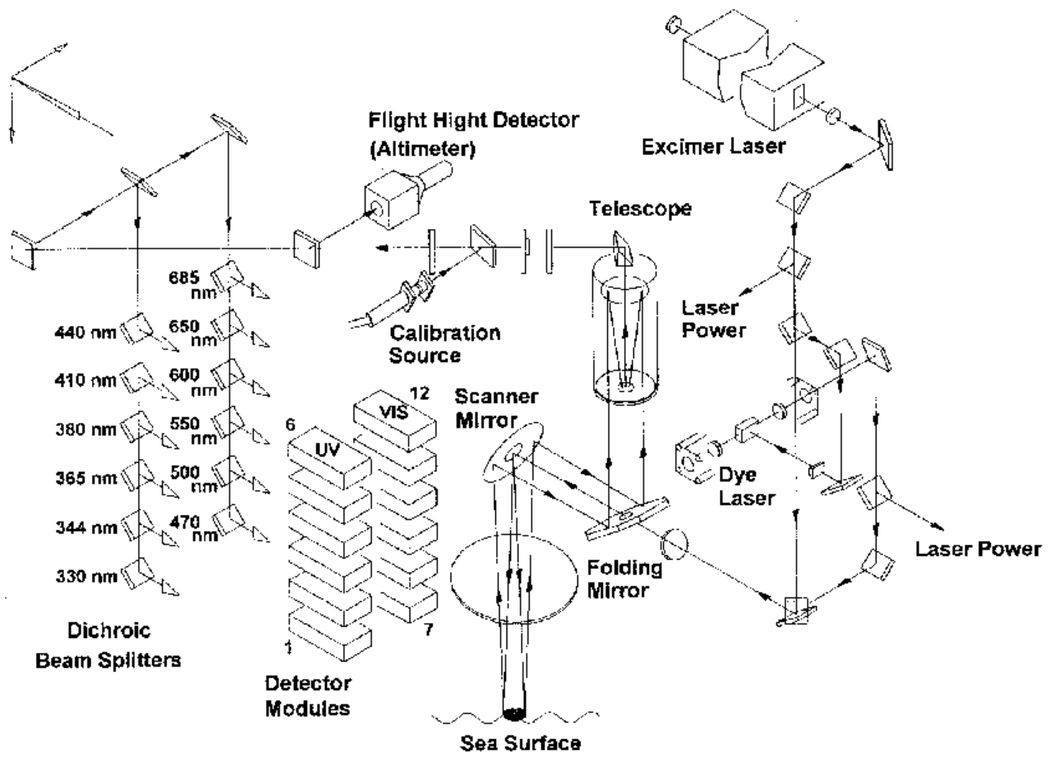

Fig. 2 - Path of rays inside the detection unit. The laser mirror in the centre part of the scan mirror deflects the laser beams to the sea surface. Fluorescent light is deflected by the main scan mirror and a fixed folding mirror to the Cassegrain telescope. The telescope output is fed via beam splitters to a flight height detector, and to 12 detection modules equipped with optical filters for wavelength selection, and photomultipliers. For a spectral calibration of the detection modules, the output light of a calibrated flashlamp is folded into the raypath behind the telescope.

- a conical scanner for two-dimensional mapping of the sea-surface (Fig. 3),
- and a VME-Bus computer for instrument control and on-line data analysis.

Since November 1993 the LFS has been operated as a component of the sensor package in a maritime surveillance aircraft. When compared with experimental lidars flown on

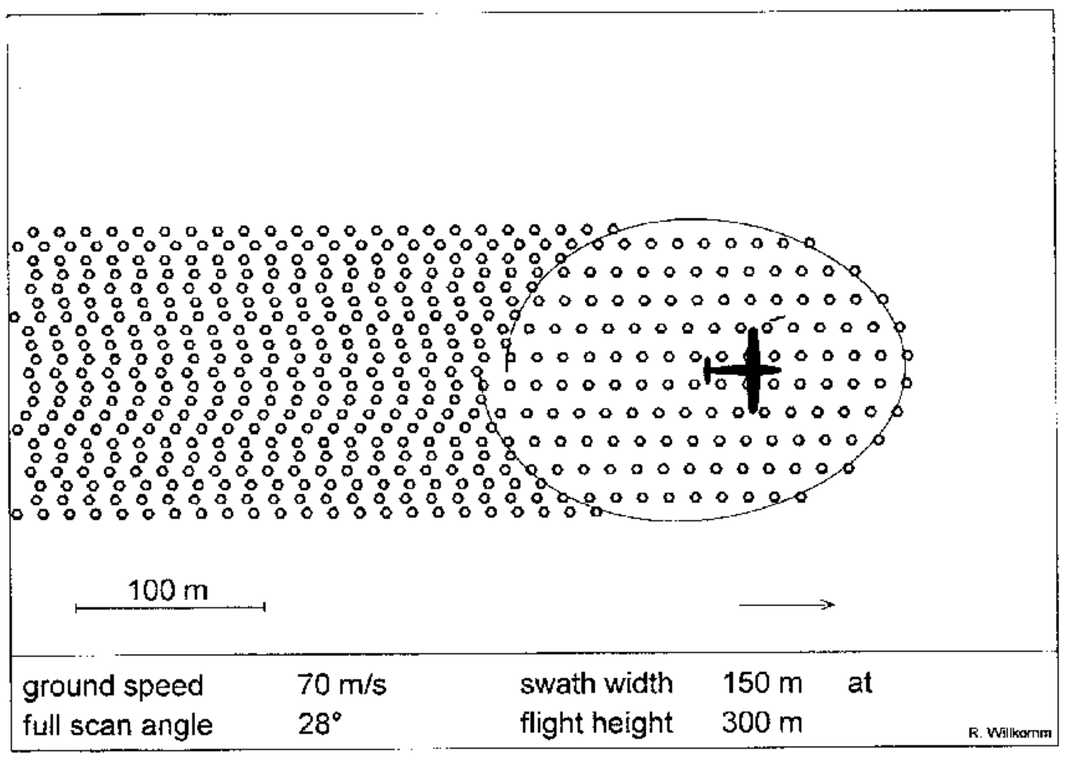

Fig. 3 - Example of a scan pixel distribution on the sea surface, obtained with a 200 Hz peak and 110 Hz average signal repetition rate of laser pulses. Laser firing is controlled by the angle encoder of the scanner. This scan pattern is used for oil spill mapping with the excimer laser, and the results presented in this paper were obtained in this operating mode. Other patterns with smaller pixel-to-pixel distance which include also dye-laser derived pixels are used for hydrographic survey, mapping of benthic algae over tidal flats, and for other applications.

board research aircraft in short-term experiments, permanent operation necessitates a number of qualification procedures, as is generally the case with avionics instruments. The prototype was therefore extensively checked in mechanical, electronic and climatic endurance tests on the ground. The mechanical safety in case of an aircraft crash was calculated. The laser output has to be eye safe when flying at the operational altitude, and the gas reservoir of the excimer laser has to withstand high pressure without losing its gas filling. The instrument is now certified for permanent aircraft use.

2. DATA ANALYSIS

Oil film thickness measurements with LFS are based on the depression of water Raman scattering from the water column in the presence of absorbing films on the sea surface. This method is broadly documented in the literature, as outlined in the introduction, and will not be further discussed here.

The accuracy of measuring the oil film thickness depends on the knowledge of the absorption characteristic of the surface film. Absorption coefficients have to be estimated from the substance type. This in turn needs to be estimated from the shape of measured fluorescence spectra if no other information on the type of oil spilled is available.

A source of systematic errors of oil volume measurements is the generally non-uniform film thickness of oil spills. Patchiness of the oil distribution within a pixel area generally leads to an underestimation of the calculated oil volume if the registered water Raman scatter intensity is taken as a measure of a presumably uniform film thickness. Errors of the volume estimation can also occur in the case of weathering, and separation of oils into fractions with different chemical and optical properties, as it has been experimentally observed (Hengstermann and Reuter, 1990). Therefore, the quality of a volume estimation depends on many factors, and the relative error will be in the range of 30 to 100% of the calculated oil volume.

An identification of substance types in surface slicks is also of particular importance for a discrimination of non-toxic and harmful matter. Such a classification of substances according to predefined classes is primarily based on the spectral variability of their fluorescence spectra. These signatures can vary with respect to shape and intensity of the spectrum. To investigate different types of oil, laboratory investigations were carried out on a representative number of samples. A catalogue of optical properties (Hengstermann and Reuter, 1992b) has been assembled from these data which is the basis for the evaluation of the classification scheme implemented into the Laser Fluorosensor. How this classification scheme has been established will be discussed below. As a result of a numerical cluster analysis performed with the spectra, nine oil classes can be identified (Fig. 4):

1: vegetable oil
2: biogenic oils, e.g. fish oil
3: light refined products, benzene
4: Diesel and lubricating oils
5: very light crude
6: light crude
7: medium crude
8: heavy crude and heavy residual oils
9: very light refined products.

The most important step when defining a classification scheme is to extract features which can be efficiently used to discriminate oil classes. The choice of these features strongly affects the design and efficiency of the classifier. It has also direct consequences on the design of the detector system, e.g. the number and spectral position of detection wavelengths. Moreover, an optimization of these features leads to a drastic reduction of the data set necessary for the classification, which then allows processing of laser fluorosensor data in near real time during overflight of oil spills. A very efficient approach for the definition of such features is the principal component analysis since it avoids the loss of important spectral information. The application of this method leads to a set of four independent features which are characteristic of each oil since they describe approximately 99% of the whole spectral information contained in the data catalogue. Each oil is then characterized by a four-tuple of numbers

$$\mathbf{v} = (v_1 , v_2 , v_3 v_4) \qquad (1)$$

For a given oil, these spectral features are then easily evaluated by inversion of a linear equation system. Another important aspect of this approach is the optimization of the

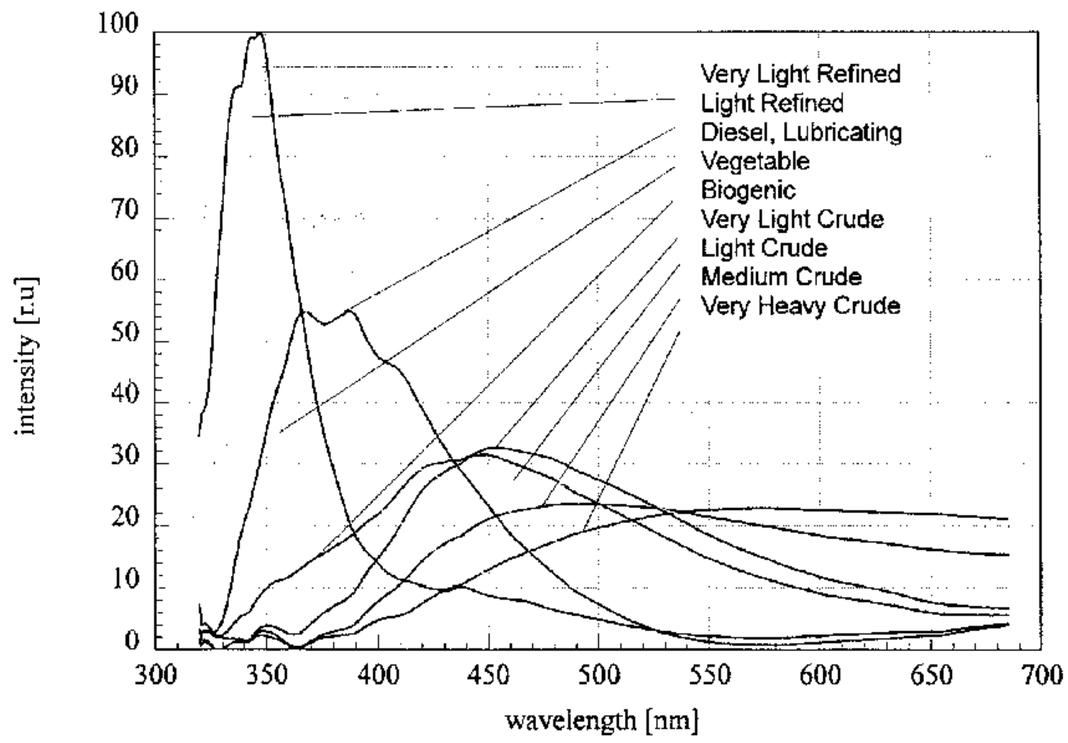

Fig. 4 - Spectral signatures of 9 oil classes derived from the catalogue of optical signatures. For better comparison the integrated fluorescence intensities are normalized to unit fluorescence efficiency.

Table 1: Laser Fluorosensor specifications.

Operating properties		
size (l x w x h)	1270 x 355 x 978 mm	excimer laser
	961 x 460 x 944 mm	detector unit
weight	315 kg	
flight height	1000 ft typ.	
electrical power	1.0 kVA	in standby
	3.4 kVA	at 110 Hz pulse rate
data interpretation in real time		
distance of eye-safe operation > 50 m		
Lasers	excimer	dye
laser medium	XeCl	polyphenyl 2
emission wavelength	308 nm	382 nm
pulse energy	150 mJ	20 mJ
pulse length	20 ns	15 ns
beam divergence	2 x 10 mrad	3 mrad
peak rep rate	220 Hz	20 Hz
max average rep rate	110 Hz	20 Hz
Telescope and scanner		
receiver telescope:	Cassegrain	
entrance aperture	20 cm	
f-number	f/10	
scanner:	conical type	
full scan angle	28° across-flight, 35° in-flight	
scan frequency	20 Hz max, selectable	
swath width	150 m	at 300 m flight altitude
pixel-to-pixel distance	10 m typ.	at 300 m flight height
		110 Hz average rep rate
Spectrograph		
number of channels	12	discrete, modular
detection wavelengths	332 - 344 - 365 - 382 - 407 - 441 nm	
	471 - 492 - 551 - 592 - 650 - 684 nm	
wavelength selection	dichroic beamsplitters, glass blocking filters and interference filters	
optical bandwidth	10 nm typ.	
detectors	compact head-on PMT, range gated	
A/D conversion	12 channel gated integrator, 11 bit resolution	

spectral layout of the detector system, as mentioned above. This concerns the number of detection channels necessary for classifying a substance from the data, and their spectral position. It can be shown that a set of five detection channels should be sufficient to evaluate characteristic features given in Eq. (1) (Hengstermann and Reuter, 1992c). In practice, more detection wavelengths are required to achieve reliable results because of signal fluctuations or experimental errors which typically occur in real measurements. The Laser Fluorosensor has been realized with twelve detection channels. They are at spectral positions which are significant when measuring oil fluorescence, but include the wavelengths of water Raman scattering and phytoplankton chlorophyll fluorescence as well.

The four-tuple in Eq. 1 can be regarded as a pattern vector $\mathbf{v}$ in a four-dimensional feature space, with v_i representing the value evaluated for the i-th feature. The classification of objects necessitates a quantitative measure of the degree of similarity or dissimilarity of objects, or classes of objects. Following the geometric interpretation of a feature space, this can be expressed as the distance between the end points of their pattern vectors:

$$d_{ij} = || \mathbf{v}_i - \mathbf{v}_j || \tag{2}$$

or

$$d_{ij} = \sqrt{\sum_{k=1}^{4} (4_{ik} - v_{jk})^2} \tag{3}$$

Oils found in a certain area of the feature space form a class of oils, and the centre of this class is defined as the average

of the feature vectors of its elements. Classification of objects by means of distances from the centres of different classes leads then to a very simple classification algorithm: the distances of an unknown oil to the centres of all oil classes are calculated, and the oil is assigned to that class with the closest distance to the centre.

In practice, a classification algorithm should also provide a measure of similarity s_{ij}, which allows to assess the quality of the result of classification. This measure will result in a value of 1 for complete correspondence with a given class j, and 0 for complete non-correspondence, in terms of distances:

$$s_{ij} = \begin{cases} 0 & d_{ij} = d_{\max} \\ 1 & d_{ij} = 0 \end{cases} \qquad (4)$$

with d_{max} denoting the distance of object i to the most distant class.

The measure of similarity defined in Equ. 4 can be considered as the probability of an object i to belong to class j. It directly follows from the distances already calculated for the classification process:

$$s_{ij} = 1.0 - \frac{d_{ij}}{d_{\max}} \qquad (5)$$

3. THE EXPERIMENT

In November 1992, a performance test was conducted in the German Bight west of the island of Helgoland, with the LFS of the University of Oldenburg and the MERES microwave radiometer developed by DLR Oberpfaffenhofen, Germany (Grüner et al., 1991). Both instruments were operated by use of a Central Operator Console from Krupp MaK Maschinenbau, Kiel, and flown in a Dornier Do 228 of the DLR Flight Department.

Following the integration of the LFS into the aircraft, the laser beam axis and telescope field of view were aligned on the ground by using a sufficiently large mirror below the bottom hatch of the aircraft which deflects the ray path to a fluorescent target at 300 m distance. The detection channels were spectrally calibrated with Nigerian light crude oil as a reference fluorophor (Hengstermann and Reuter, 1992b) . Finally, the basic electronic and optical functions of the instrument were checked in a test flight over water.

Hydrographic measurements were made in parallel to the flights on board the oil combatting vessel MS "Mellum" of the Federal Special Unit for the Abatement of Oil Pollution, Cuxhaven. Substances were also discharged by this ship (Table 2). Meteorological parameters like wind speed and sea state were measured, and hydrographic *in situ* data of temperature and salinity were gathered with a submersible probe (Model OTS, ME Meerestechnik-Elektronik GmbH, Trappenkamp, Germany). Fluorescence spectra of water and oil samples were obtained with a laboratory spectrofluorometer (Perkin Elmer Model LS 50) which was also installed on board the ship.

The weather was not favourable throughout the experiment, with wind of 11 to 17 m/s (6 to 8 Bft) from south to west. These conditions were beyond the predefined range of wind speeds for the performance test. Despite this, a first flight was effected on November 4, 1992, and gas oil discharged by MS "Mellum" could be successfully analyzed. After a standby period of 5 days with continuously bad weather, it was decided to perform the other flight operations on 9-11 November (Table 2). In practice, no limitations occurred for the measurement of larger oil volumes, and only the detec-

Table 2: Dates and position of MS "Mellum" during the discharge of oils; wind conditions and hydrographic data.

Date	Time (UTC)	Substance Type & Volume	Latitude Longitude	Water Depth	Wind Speed & Direction	Water Temp.& Salinity
4 Nov 92	14:10	gas oil 0.2 m^3	54°24.6' N 7°22.3' E	30 m	16 m/s 280°	11.4 °C 33.8‰
9 Nov 92	10:25	slop oil 2.5m^3	54°04.2' N 7°20.1' E	35 m	12 m/s 170°	10.2 °C 33.28‰
9 Nov 92	11:43	gas oil 0.2 m^3	54°04.6' N 7°18.6 'E	35 m	11 m/s 170°	10.0 °C 33.26‰
9 Nov 92	14:25	crude oil 5.0 m^3	54°04.4' N 7°15.5' E	33 m	11 m/s 170°	10.0 °C 33.18‰
9 Nov 92	15:18	bilge oil 60 l/n.m.	54°04.5' N 7°12.2' E	33 m	11 m/s 170°	9.9 °C 33.2‰
10 Nov 92	10:10	slop oil 120 l/n.m.	54°04.6' N 7°17.3' E	30 m	16 m/s 260°	10.3 °C 33.6‰

tion of small quantities in the order of 100 litres per nautical mile discharged from the moving ship was difficult or even impossible because of the rough sea state.

During flights over oil spills a nadir-looking VHS camera allowed for a direct observation of the sea surface. Although the quality of the video system is not perfect, the availability of these images proved very helpful when processing and interpreting the LFS measurement on the ground.

During processing the data the 365 nm detection channel was found to have an unstable sensitivity during the measurements, and the channel was not considered any longer. However, this detection wavelength is important for the substance classification, and for estimating the 344 nm water Raman scatter intensity from which the oil film thickness is derived. Therefore, the 365 nm signals were simulated by interpolating the 332 and 382 nm signals to that wavelength. We assume that the possible loss of accuracy of the calculated film thickness still remains in the range which is to be expected, as given in section 2.

Following the interpretation of the raw data in terms of film thickness and substance type, the results were further processed with Microsoft Excel, which allows for an easy presentation of two-dimensional maps of oil spills on the sea surface, as obtained with the scanning operation of the LFS. Except for a rejection of outliers which may occur by an incorrect time gating of the detectors or laser trigger, no attempts have been made to average or filter the data for noise reduction, and the elements of each image correspond to individual signal returns.

Film thickness distributions have been calculated from the intensity of water Raman scattering. The absorption coefficient of the oils has been thoroughly set to 1 μm^{-1}. A more correct interpretation of the film thickness data shown below would make use of values of the absorption coefficients which have been measured on samples, or estimated from a data catalogue. This has not been considered, since realistic values of the absorption coefficient might deviate by a factor of two from the value 1 μm^{-1} adopted here, which is still in the order of accuracy of the method. Therefore, the data presented here are equivalent to the dimensionless optical depth of the oil film, i.e. the product of absorption coefficient and film thickness of the oil.

4. RESULTS

4.1 Gas oil

On 4 November 1992, discharge and spreading of a gas oil spill could be completely traced with LFS measurements. The spill consisted of 0.2 m^3 fuel oil of MS "Mellum". This light refined oil is characterized with high fluorescence yield at UV and blue wavelengths, which allows for a very sensitive detection with fluorescence spectroscopy. The oil spreads rapidly over the sea surface and loses its volume fast due to evaporation.

Following the injection at 14:10 h the spill spread fast, covering an area of about 200 to 50 m in size at 14:15 h (Fig. 5) and 300 to 100 m at 14:19 h (Fig. 6). The oil-covered area increased further, while those portions with a film thickness above 10 micrometer became smaller (14:29 h, Fig. 7) and disappeared. Only small spots of increased film thickness were visible in the LFS data 40 minutes after discharge, and the enhanced daylight reflection of the oil film which was easily visible in the video image until then had almost disappeared (14:51h, Fig. 8). A complete sequence of LFS data is shown in Fig. 9, which describes the evolution of the gas oil spill in detail.

The substance classification makes use of the fluorescence spectra measured inside the oil spill at positions with highest optical thickness of the surface film. Fig. 10 gives two examples of these spectra taken shortly after discharge and near the end of the overflights. In spite of the marked reduction of emission intensity with time, the spectral shape shows little variation. Therefore, the results of the substance classification are very stable in all overflights (Table 3), and yield Diesel and lubricating oil as the substance with closest similarity to the fluorescence signature. As with the thickness images of the gas oil slick shown in Fig. 9, images of the similarity of the gas oil spill with that class of substances are displayed in Fig. 11.

A second gas oil spill was produced on 9 November 1992. Oil type and volume were identical with the spill investigated on the 4th November. Airborne measurements with the LFS are consistent with the data measured earlier. Therefore, these results are not shown, except for the substance classification given in Table 4, which again yields a good agreement with the class of Diesel and lubricating oils.

4.2 Slop oil

On 9 November 1992, slop oil was released at 10:25 h with a quantity of 2.5 m^3. This oil sample consisted of an emulsion of different oils and water. The oils had been collected from the sea surface during clean-up operations by MS "Mellum". Detailed chemical and physical characteristics of the oil were not available.

Discharge was made in a short period of time, and therefore the bulk of the oil remained concentrated in a small spot with a size of about 100 to 50 m. Because of wind speeds of 12 m/s, a smaller volume of the oil which emerged from the spot was spreading over large areas of the sea, giving rise to a thin film with silvery colour. This film is hardly visible in the video images, the LFS data display a thickness of about 0.5 µm in these areas (Fig. 12).

Table 3: Gas oil spill, 4 Nov 1992. Probability values of similarity s_{ij} according to Equ. 5 with the given classes of substances.

	..... Time of overflight, 4 Nov. 1992					
substance class	**14:15 h**	**14:19 h**	**14:24 h**	**14:29 h**	**14:34 h**	**14:44 h**
vegetable oil	.47	.44	.45	.49	,.41	.31
biogenic oil	.47	.42	.43	.45	.38	.32
light refined	.21	.21	.21	.21	.21	.20
Diesel, lubricating oil	.75	.78	.77	.73	.82	.82
very light crude	.33	.29	.29	.31	.25	.20
light crude	.34	.32	.32	.33	.30	.26
medium crude	.31	.30	.30	.30	.30	.29
heavy crude	.17	.20	.19	.17	.22	.26
very light refined	.00	.00	.00	.00	.00	.00

The emission spectrum of the oil (Fig. 13), measured at the thickest part of the spill, yields a much lower signal intensity compared with the gas oil spectrum, as is expected. Fluorescence covers the entire visible spectrum, with a pronounced maximum at blue wavelengths. With this spectral behaviour, the oil is classified as light or very light crude (Table 4). The similarity of the spill with these classes of substances outside the spot where the bulk of the oil is concentrated, is relatively low, with values of 0.5, typically (Fig. 14). This result might be due to the presence of signals from the water column below the oil. However, evaporation of fluorescent compounds and hence a loss of the characteristic fluorescence spectrum certainly contributes to this result as well.

Table 4: Slop oil, gas oil and crude oil spills, 9 Nov 1992. Probability values of similarity sij according to Equ. 5 with the given classes of substances.

	..... Oil spill and time of overflight, 9 Nov. 1992			
substance class	**slop oil 11:28 h**	**slop oil 11:32 h**	**gas oi1 12:00 h**	**crude oil 15:04 h**
vegetable oil	.44	.45	.35	.21
biogenic oil	.45	.44	.41	.28
light refined	.20	.21	.22	.16
Diesel, lubricating oil	.32	.38	.90	.29
very light crude	.77	.73	.28	.22
light crude	.76	.73	.36	.46
medium crude	.56	.56	.39	.68
heavy crude	.20	.22	.32	.84
very light refined	.00	.00	.00	.00

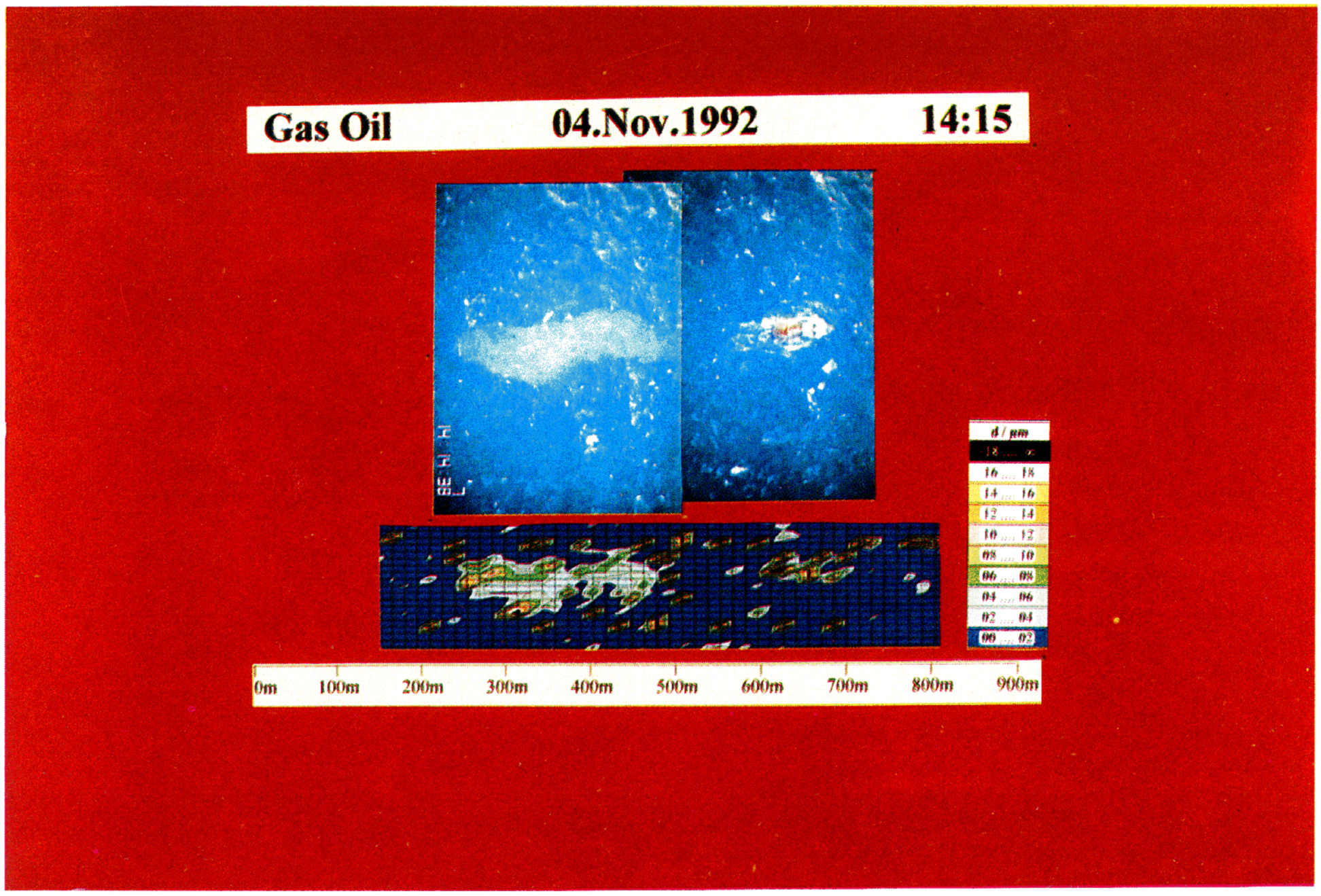

Fig. 5 - Gas oil spill on 4 Nov 92, 14:15 h, 5 min after discharge. LFS data (below) are compared with images taken with the nadir-looking video camera (above). LFS data correspond to the film thickness in micrometre at pixels defined by individual laser shots as shown in Fig. 3. The distance scale given below holds for the along-track and across track direction of the LFS thickness map, and for the video image. The ship to the right of the spill apparently leads to a reduction of water Raman scatter, resulting in an increased "film thickness" in the LFS image at the position of the ship. The small patches with green and yellow colours are due to white caps, which depress the water Raman scatter signal from the water column as well.

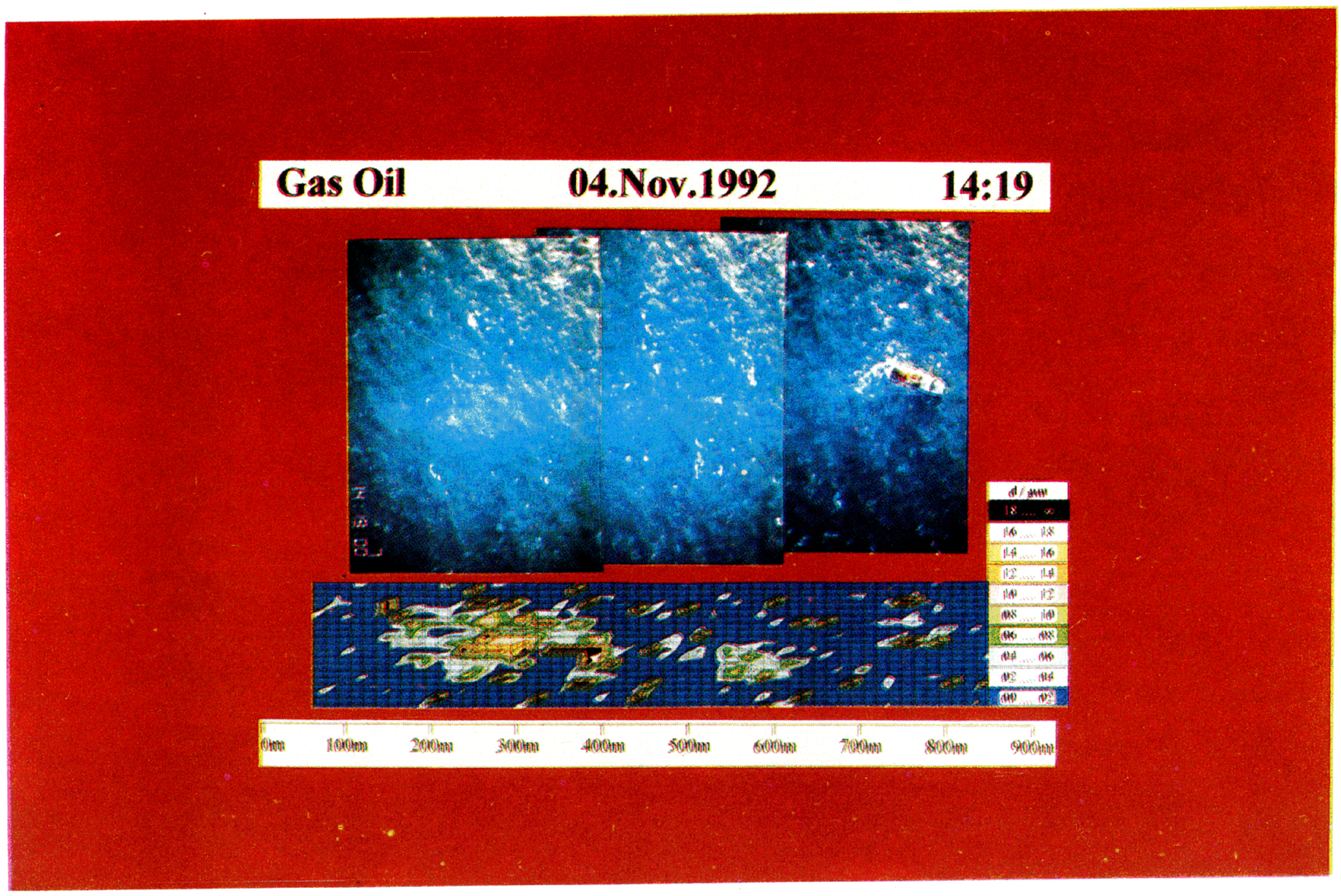

Fig.6 - Film thickness of the gas oil spill on 4 Nov 92, 14:19h, 9 min after discharge. A second smaller spill is apparent in the video and LFS images at position 570 m, the ship position is 670 m.

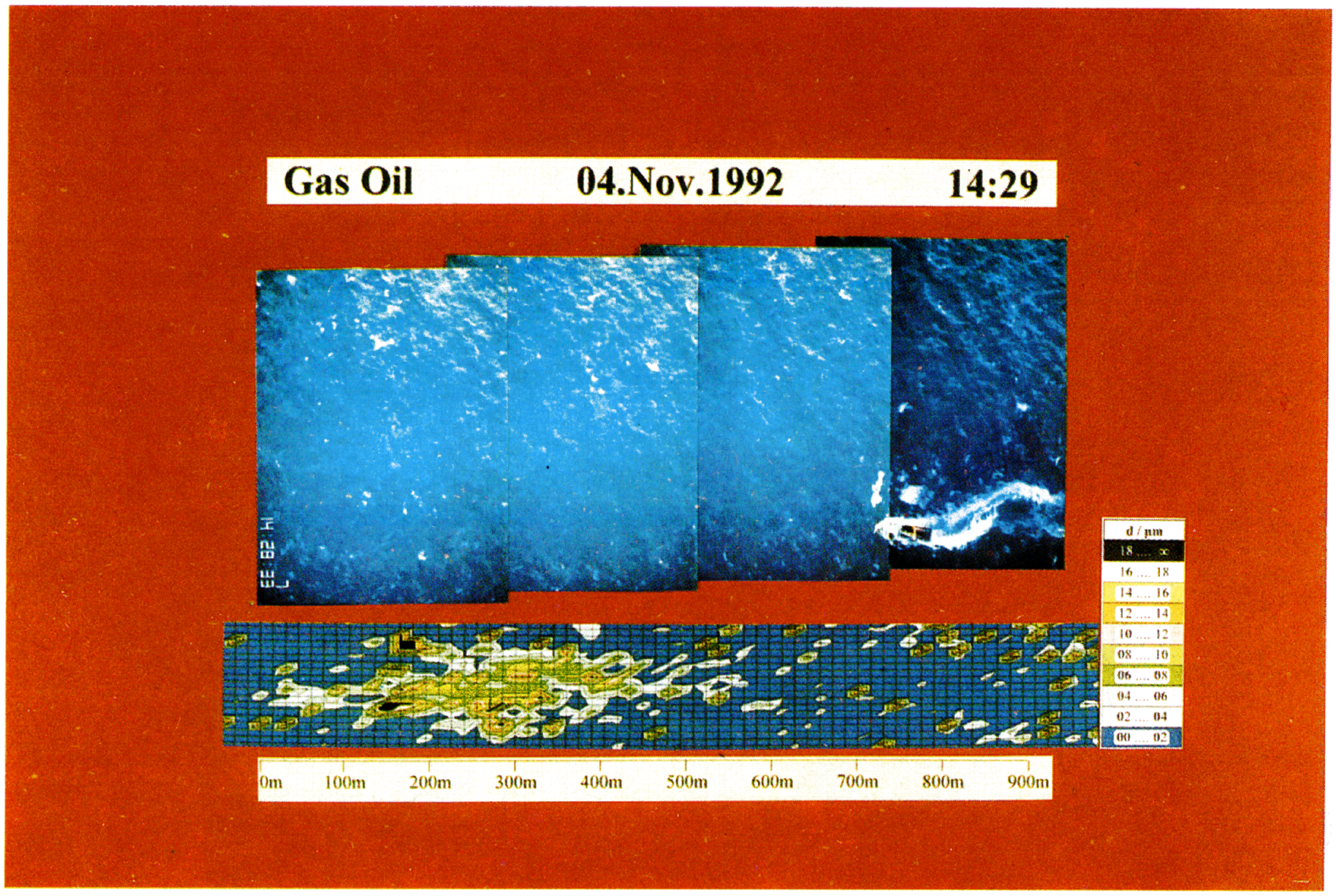

Fig. 7 - Gas oil spill on 4 Nov. 92, 14:29 h, film thickness distribution 19 min after discharge. The ship is outside the area covered by the LFS scan width.

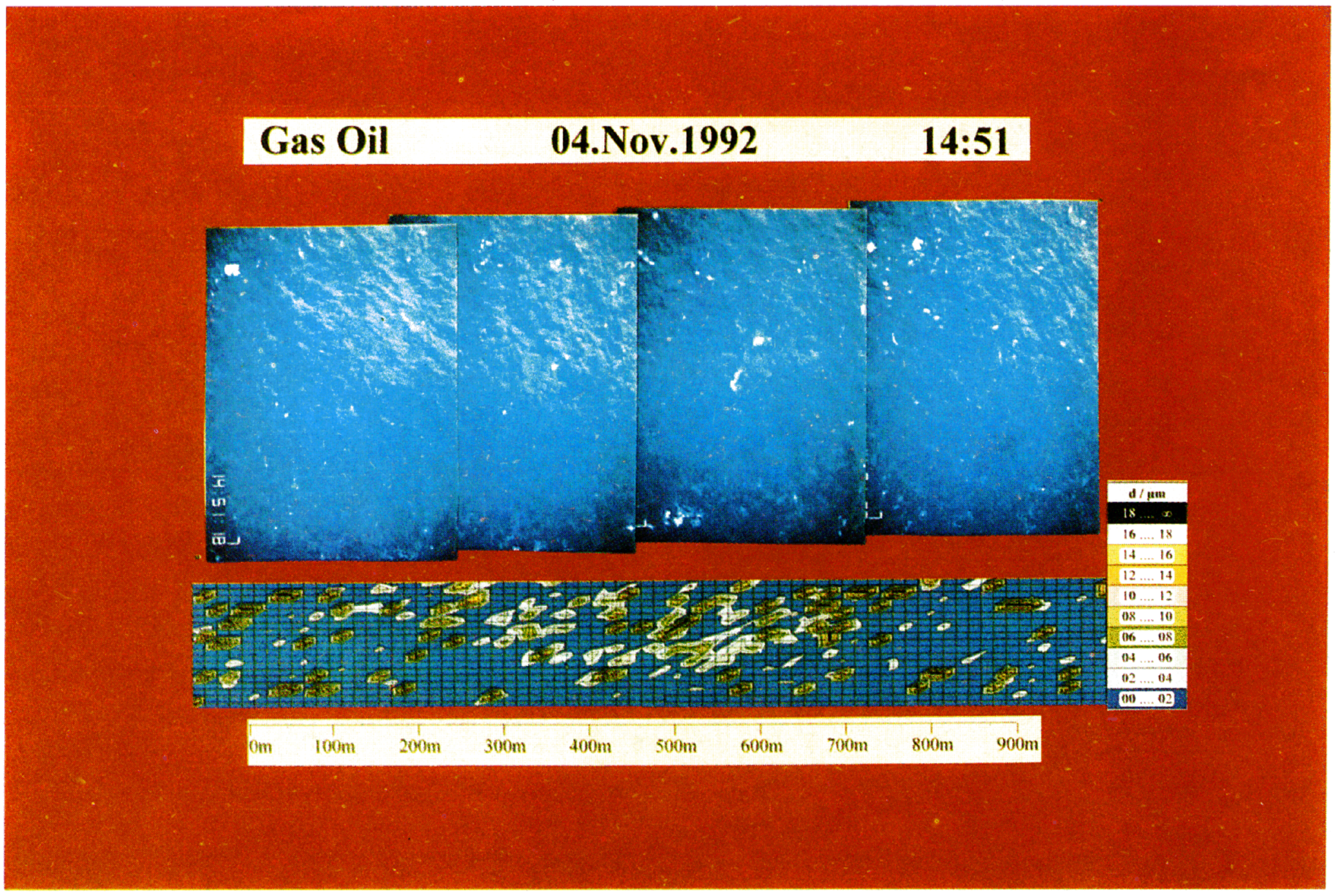

Fig. 8 - Gas oil spill on 4 Nov 92, 14:51 h, film thickness distribution 41 min after discharge. Only weak signals are registered in both the LFS data and the video image.

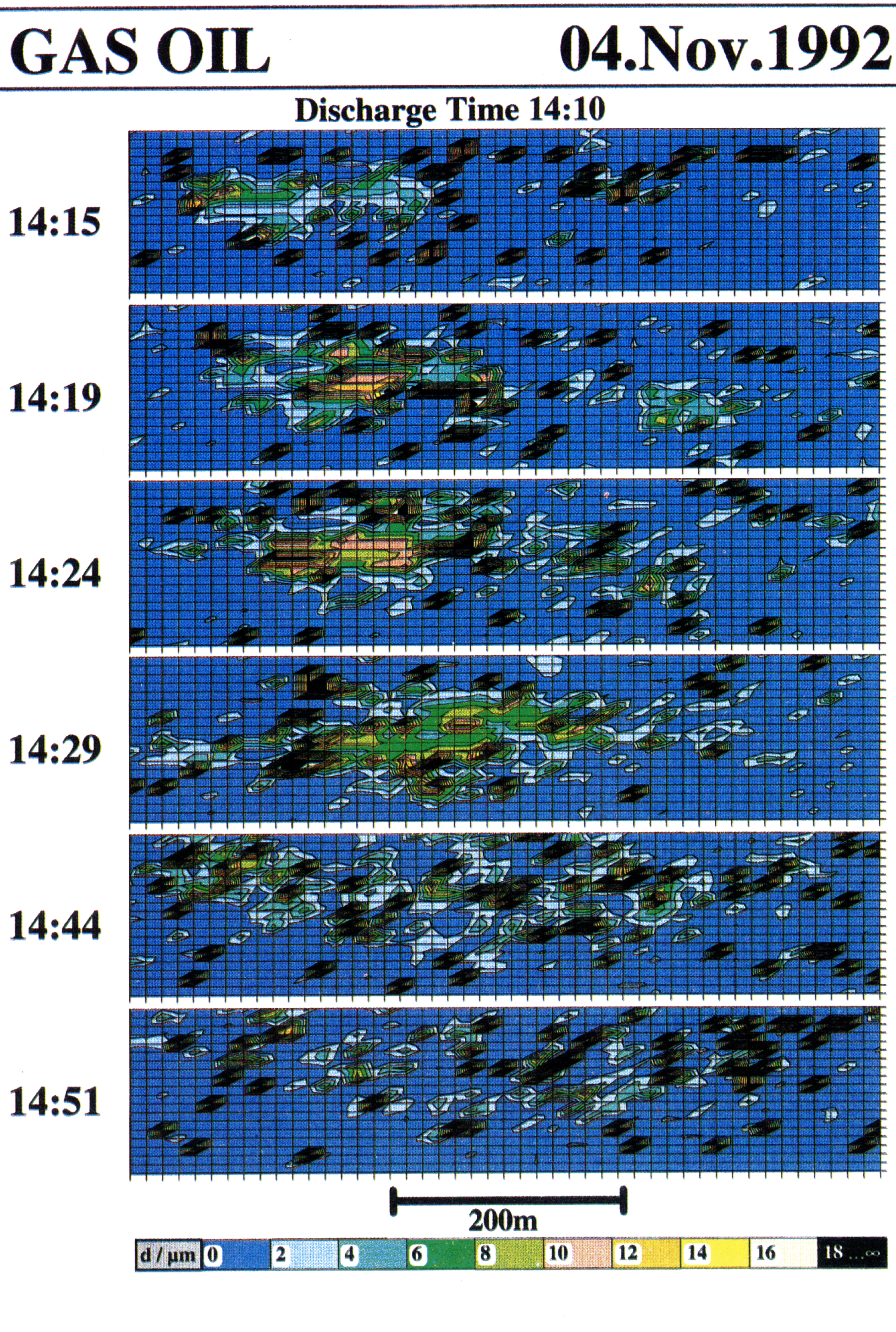

Fig. 9 - Sequence of six overflights of the gas oil spill on 4 Nov. 92, showing the film thickness distribution.

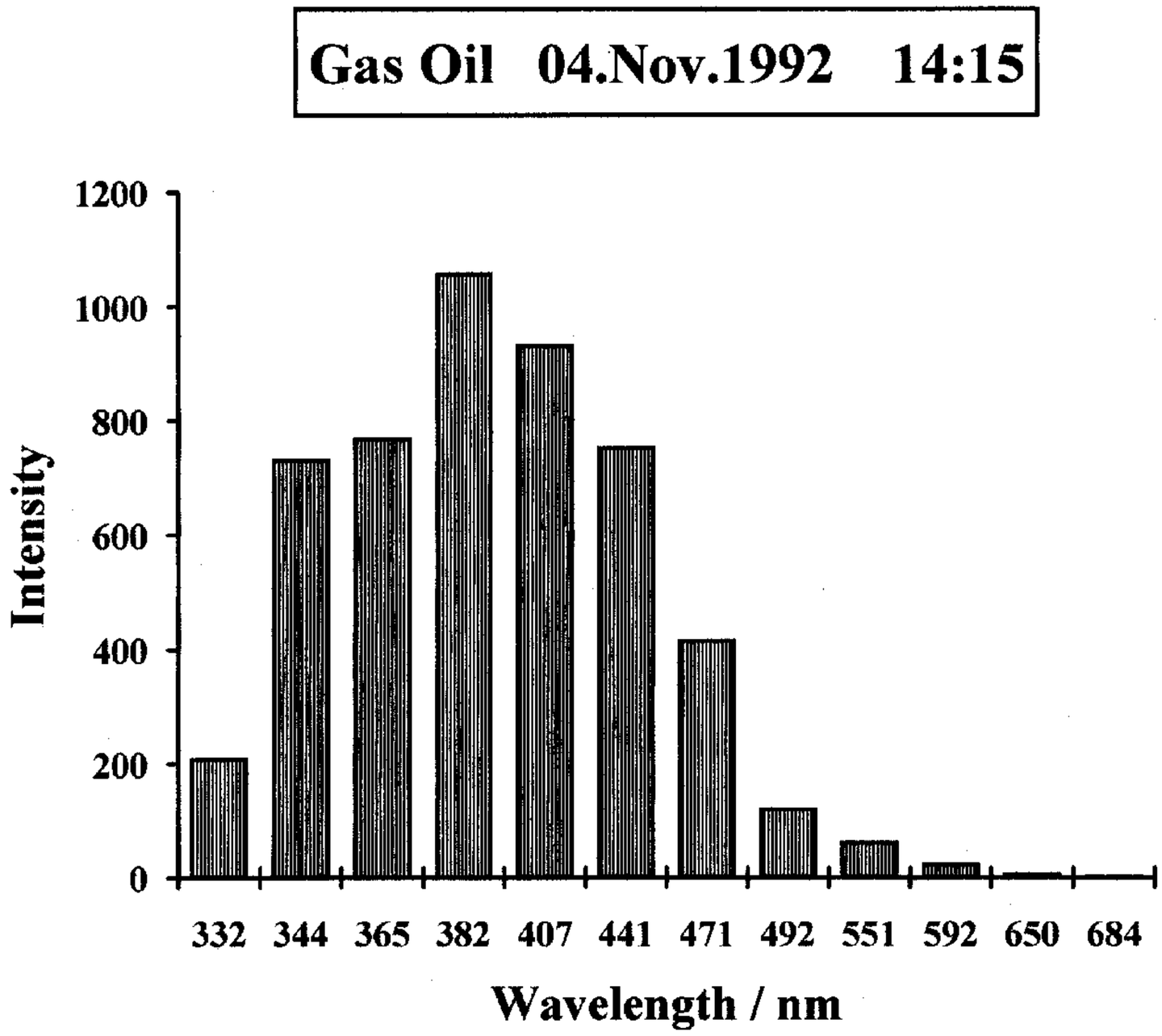

Fig. 10 - Emission spectra of the gas oil spill on 4 Nov 92 at 14:15 h (a) and 14:44 h (b) taken at the thickest parts of the surface film. The abscissa is not a wavelength scale, but denotes detection channels and their centre wavelengths.

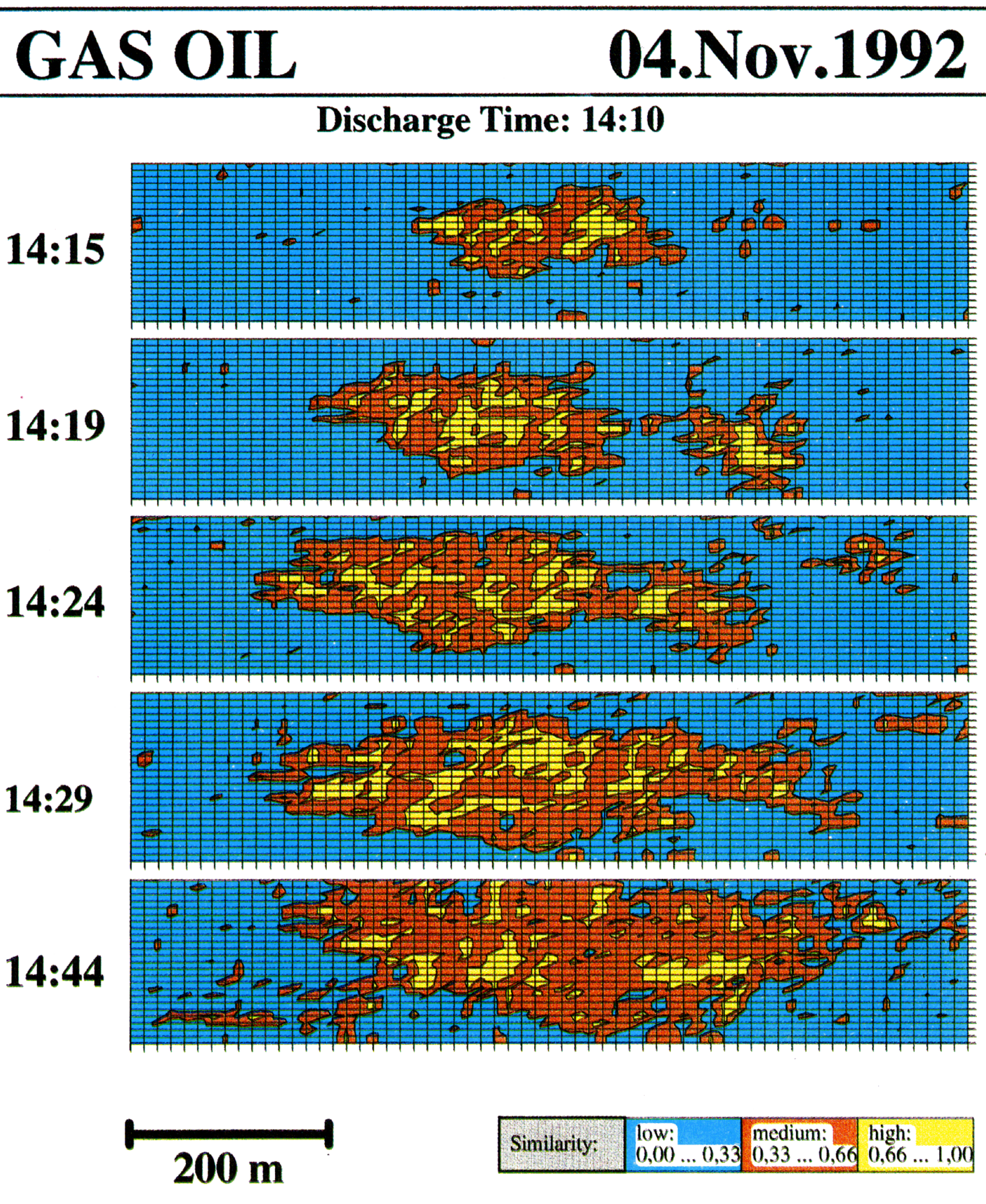

Fig. 11 - Sequence of five overflights of the gas oil spill on 4 Nov 92, showing the similarity of the emission spectra with the fluorescence signature of Diesel and gas oil as defined in Equ. 5.

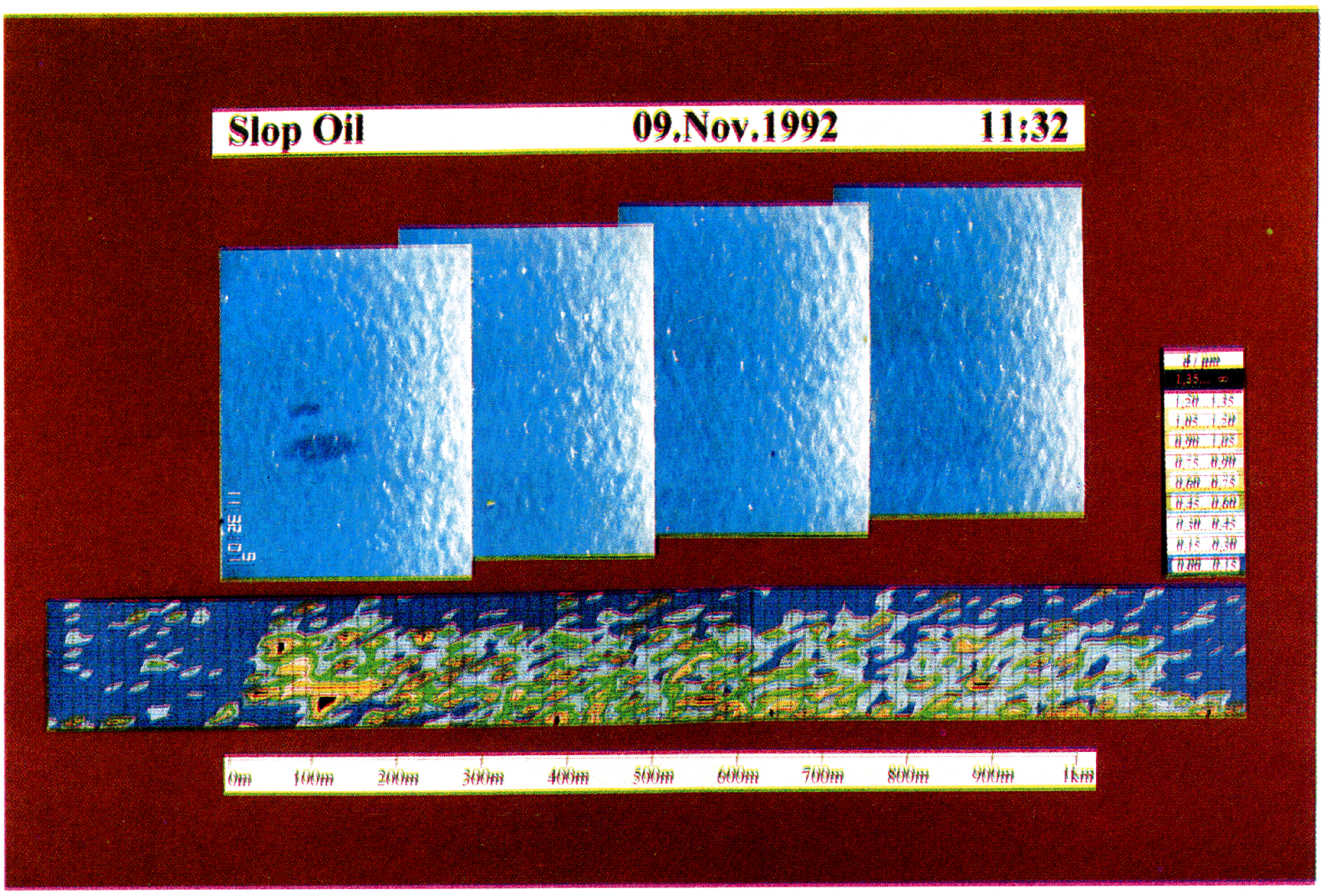

Fig. 12 - Slop oil spill on 9 Nov 92, 11:32 h, film thickness distribution. LFS data (below) are compared with images taken with the nadir-looking video camera (above). The thin film emerging from the bulk of the oil at position 100 m of the flight track is sensitively measured with the LFS, but scarcely visible in the video image.

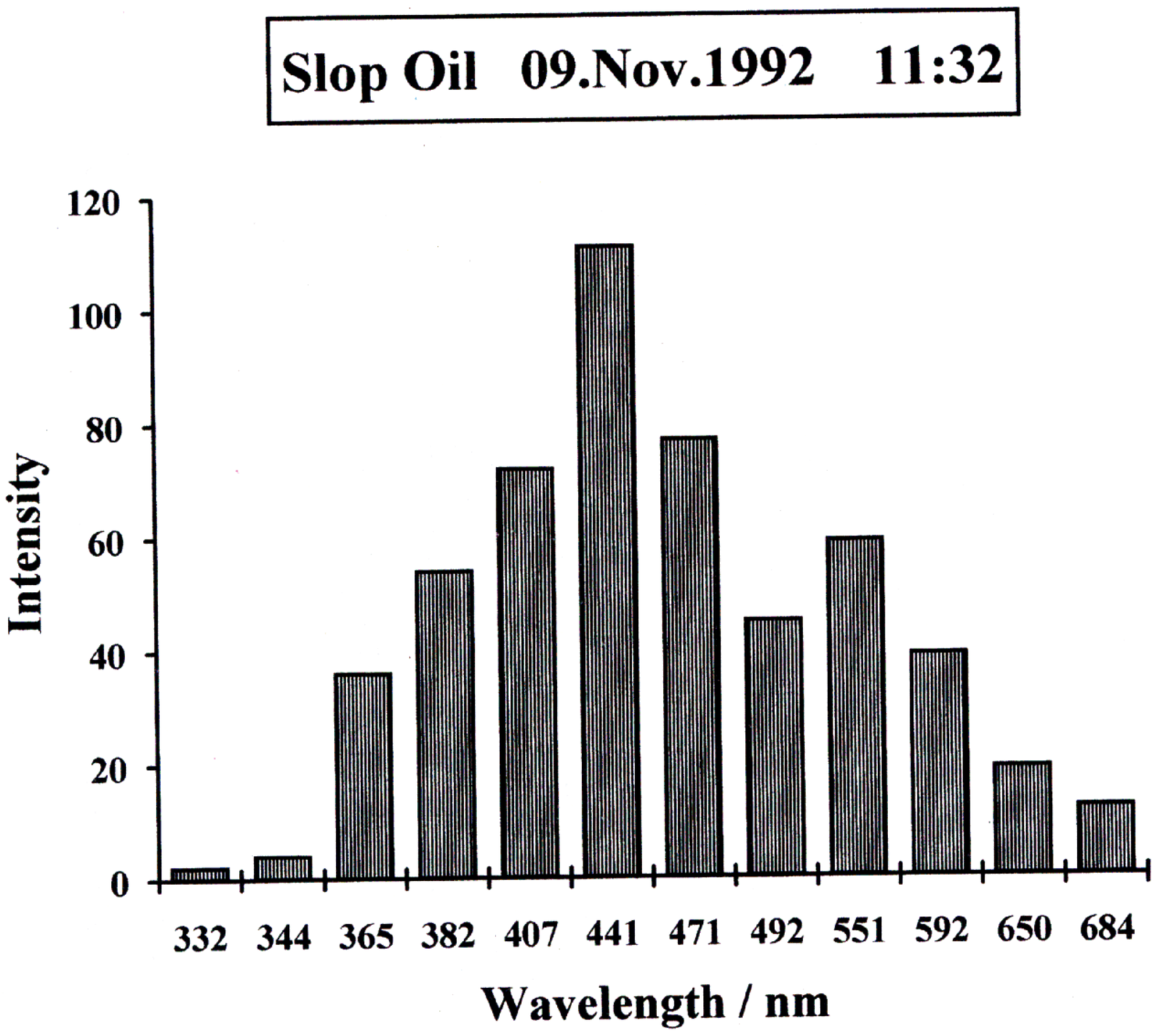

Fig. 13 - Slop oil emission spectrum taken at the thickest part of the spill, 9 Nov 92, 11:32 h.

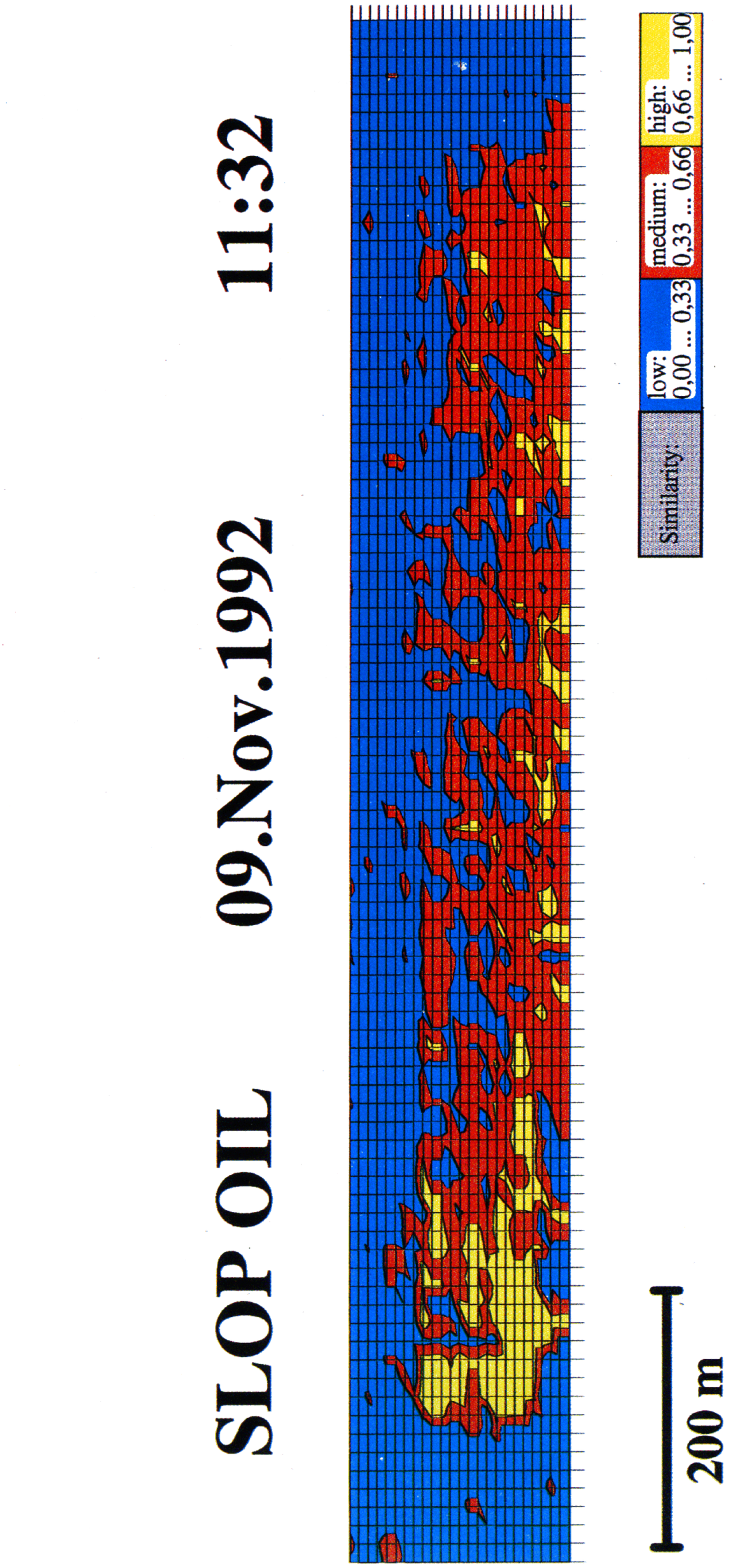

Fig. 14 - Slop oil spill on 9 Nov 92, 11:32 h, similarity with the signature of very light crude oil.

4.3 Crude oil

On the same day, a 5 m^3 crude oil spill was produced following the slop oil spill. The oil was a heavy crude, its origin is Middelplate in the German part of the Wadden Sea. Discharge was made from the moving ship, resulting in a large oil-covered area on the sea surface. Fig. 14 gives an impression of the shape and dimension of the spill 30 min after release.

The film thickness distribution measured with the LFS displays well those areas where a film in the order of 1 µm thickness is present. Spots with large oil volumes which are clearly visible in the video image, cannot be identified with the LFS. This is due to the high absorption characteristic of the crude oil in the ultraviolet, resulting in optically thick layers already in the presence of films with a few micrometres thickness.

The emission spectrum (Fig. 16) corresponds well with the signature which is to be expected with heavy crude: a very low fluorescence intensity compared with lighter oils, and a dominance of the red portion of the spectrum. This is also supported by the result of the substance classification (Table 4). The similarity with the heavy crude oil signature attains high values also in those parts of the spill where films with only a micrometre thickness are found (Fig. 17). This is again due to the strong absorption coefficient of the oil, which gives rise to an emission of the oil-specific spectrum already in the presence of these very thin films. .

DISCUSSION

As a result of the LFS development an instrument is available which is qualified for permanent installation on board an aircraft, and which meets the operational specifications for long-term use in maritime surveillance. When compared with nadir-looking lidars utilized earlier, the use of a scanner and a laser with high pulse firing rate yields two-dimensional maps of the sea surface, and this provides a powerful tool when analyzing oil spills and other structures on the ground with comparably small geometric scales.

The experimental results described in this paper demonstrate the performance of the LFS. Several oil spills were analyzed, and maps of their film thickness distribution could be derived. In principle, these maps provide a means to estimate the quantity of oil observed along the flight track. However, no attempt has been made to derive the total oil volume of these spills: the presence of spots with films in the order of a millimetre thickness which are far beyond the dynamic range of the method, does not allow to estimate these volumes.

In the same experiment, two spills were produced with much smaller volumes of oil which should be within the range of film thickness measurements with fluorescence lidar. These spills were easily visible on the sea surface because of their wave-damping effect. However, it was surprising to see that they could hardly be detected with the LFS, in contradiction to earlier experiments with similar spill volumes (Hengster-

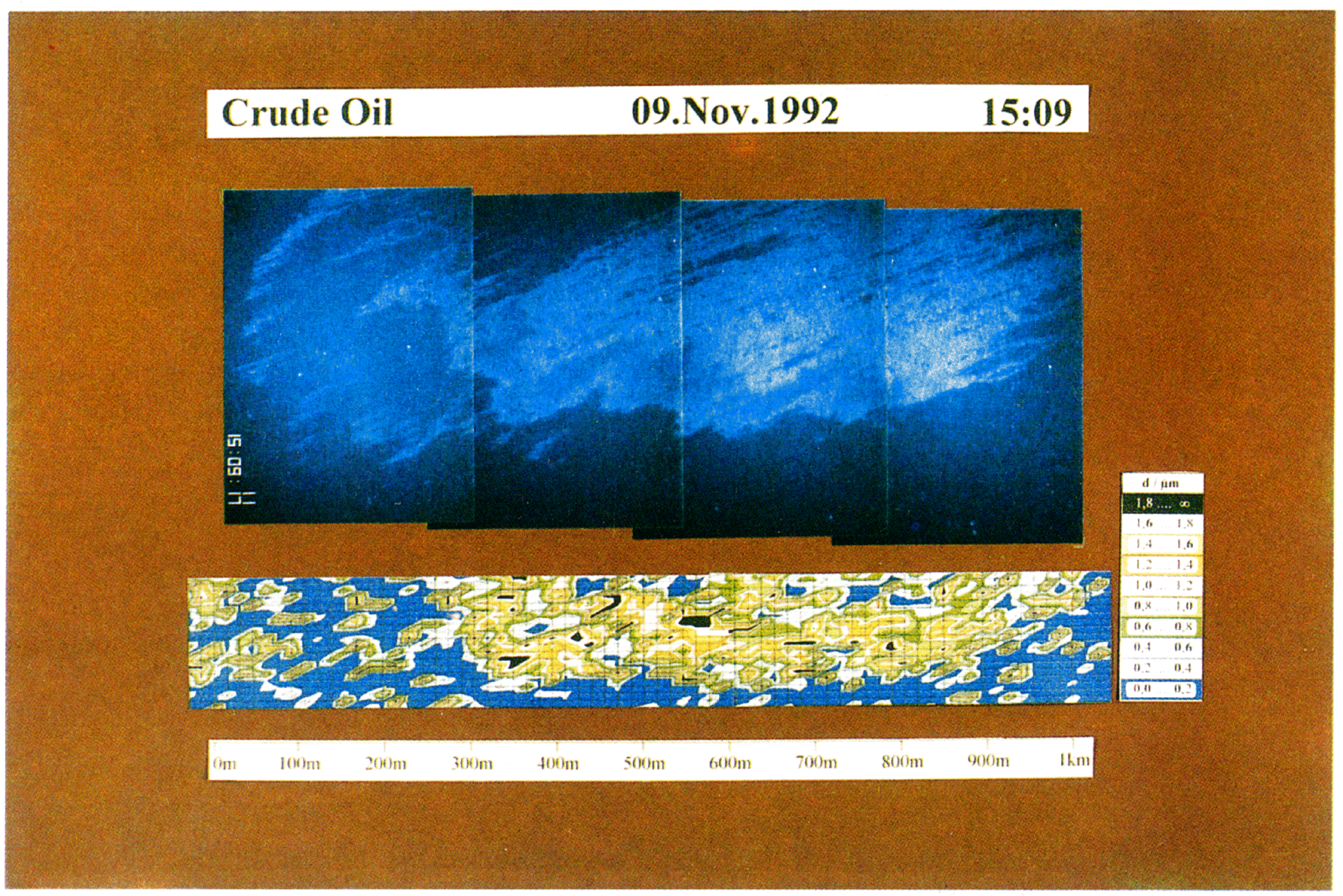

Fig. 15 - Crude oil spill on 9 Nov 92, 15:09 h, film thickness distribution.

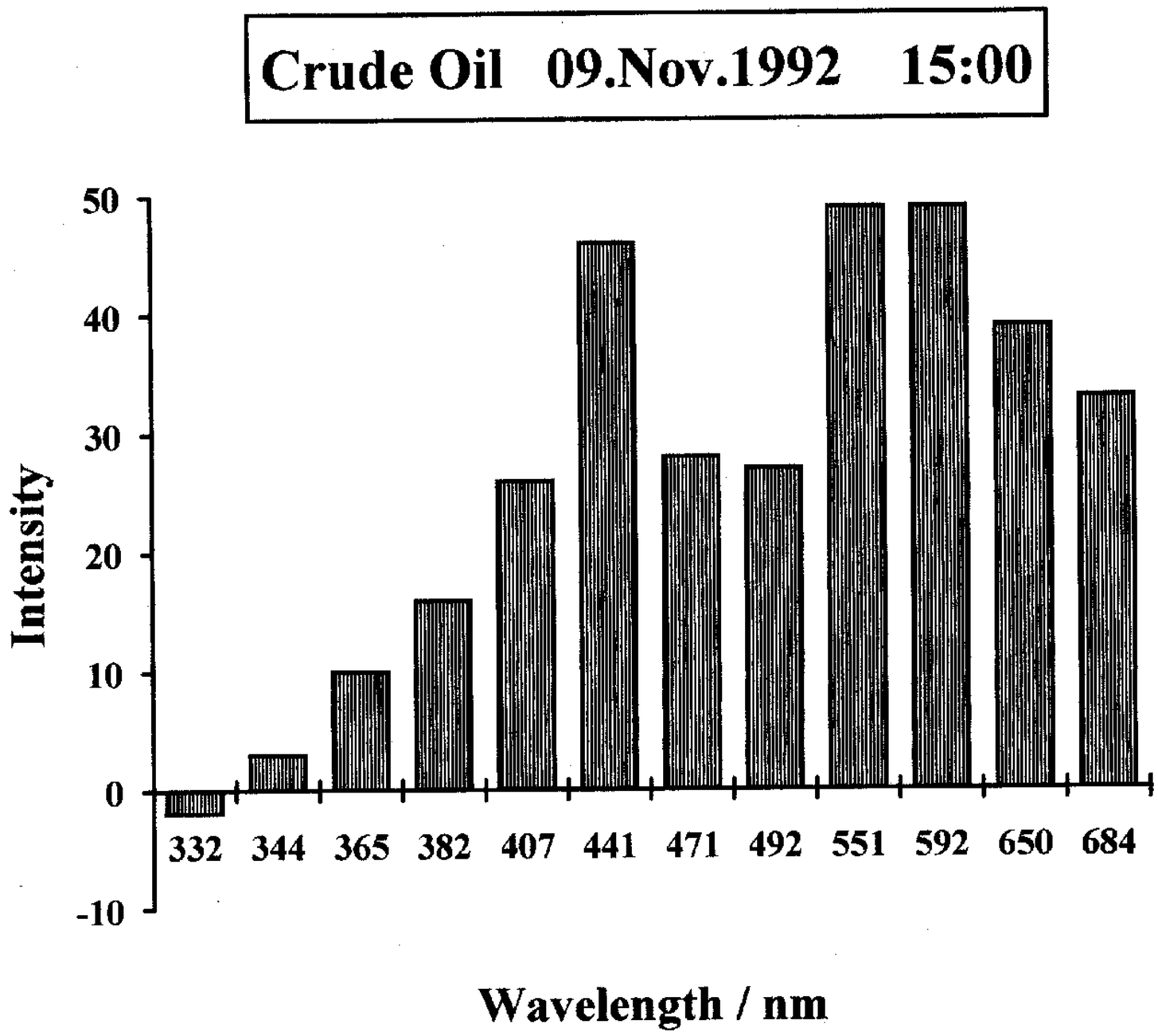

Fig. 16 - Crude oil emission spectrum taken at a thick part of the spill, 9 Nov 92, 15:00 h.

mann and Reuter, 1990). We assume that strong winds and hence a rough sea state - beyond the weather conditions specified for airborne surveillance operations - with fast evaporation of fluorescent compounds were responsible for the poor signals from these spills. It could be shown in a flight campaign in 1993 that a mapping of oil spills with a discharge rate of 30 litres per nautical mile is possible in case of calmer weather conditions, yielding results of the same quality as the data shown here. Because of a film thickness of less than a few micrometres, a volume estimation was meaningful in these cases, and the result was in good agreement with the volume of oil discharged by the ship.

The classification of oils on the basis of a principal component analysis is another important feature of the LFS. It allows to drastically reduce the number of detection wavelengths required for gathering significant information from oil spills. Because of the low number of data, the classification can be performed very rapidly, and this opens a way to interpret the data in real time, i.e. during the overflight of an oil spill, which is an important aspect in maritime surveillance.

The substance classification performed with the data of the performance test described in this paper yields results which are consistent with the discharged oil types. The classification performed over optically thick films remains stable in repeated flights. A degradation of the classification process should occur in the presence of thin oil layers; in such cases the data can be improved with a non-linear approximation which allows extraction of the characteristics of the oil (Hengstermann and Reuter, 1992c). This approximation has not yet been integrated into the algorithms available for data interpretation at the time of this experiment. The results presented here show that in practice the similarity of the oil with the oil class identified over optically thick films is still high in the presence of thin layers, if weathering of the oil and subsequent changes of its optical properties are negligible. The method is hence stable also in the case of small fluorescence contributions from other substances, e.g. gelbstoff in the water column below an oil spill.

With the permanent availability of the LFS for maritime surveillance the data basis of fluorescence properties of oils and the number of airborne measurements over oil spills will be considerably enlarged in future. We expect that this will provide a chance to gain much better experience with the interpretation of signals from oil spills when compared with the few airborne experiments performed previously. This will lead to a continuous improvement of the method of analyzing maritime pollution with laser fluorosensors.

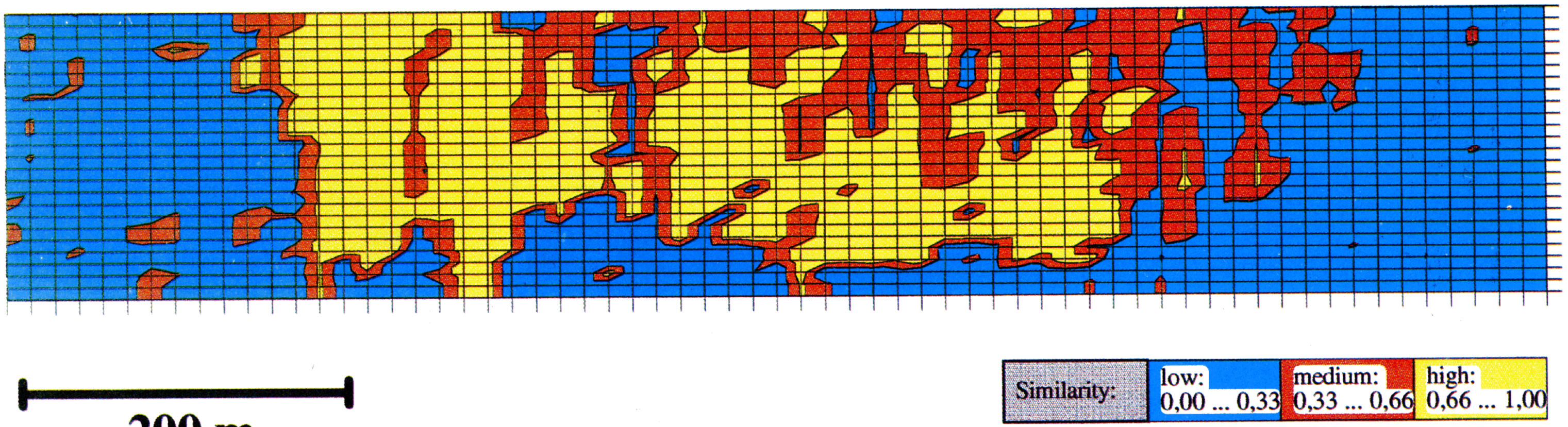

Fig. 17 - Crude oil spill on 9 Nov 92, 15:04, similarity with the signature of heavy crude oil.

ACKNOWLEDGEMENTS

Development of the Laser Fluorosensor was financially supported by the DLR Project Executive Department Environmental Protection and Technologies, Bonn, on behalf of the Federal Ministry for Research and Technology. Essential parts of the mechanical and electric structure, and the computer equipment, were realized in cooperation with Krupp MaK Maschinenbau, Kiel, in 1989-92, and by the mechanical and electronics workshops of the University of Oldenburg, which is gratefully acknowledged. We are also grateful to DLR Oberpfaffenhofen for making available the DO 228 research aircraft used in the experiment, and to the Federal Special Unit for the Abatement of Oil Pollution, Cuxhaven, for supporting the experiment with MS "Mellum".

REFERENCES

Bristow, M., Bundy, D., Edmonds, C.M., Ponto, P.E., Frey, B.E., and Small, L.F., 1985, Airborne laser fluorosensor survey of the Columbia and Snake rivers: simultaneous measurements of chlorophyll, dissolved organics and optical attenuation. International Journal of Remote Sensing, 6, 1707-1734.

Burlamacchi, P., Cecchi, G., Mazzinghi, P., and Pantani, L., 1983, Performance evaluation of UV sources for lidar fluorosensing of oil films. Applied Optics, 22, 48-53.

Dudelzak, A., Babichenko, S., Poryvkina, L., and Saar, K.J., 1991, Total luminescent spectroscopy for remote laser diagnostics of natural water conditions. Applied Optics, 30, 453-458.

Exton, R.J., Houghton, W.M., Esaias, W., Harriss, R.C., Farmer, F.H., and White, H.H., 1983, Laboratory analysis of techniques for remote sensing of estuarine parameters using laser excitation. Applied Optics, 22, 54-64.

Grüner, K., Reuter, R., and Smid, H., 1991, A new sensor system for airborne measurements of maritime pollution and of hydrographic parameters. GeoJournal, 24.1, 103-117.

Hengstermann, T., and Reuter, R., 1990, Lidar fluorosensing of mineral oil spills on the sea surface. Applied Optics, 29, 3218-3227.

Hengstermann, T., Loquay, K.D., Reuter, R., Wang, H., and Willkomm, R., 1992a, A laser fluorosensor for airborne measurements of maritime pollution and of hydrographic parameters. EARSeL Advances in Remote Sensing, 1, 85-90.

Hengstermann, T., and Reuter, R., 1992b, Optical Spectra of Fluorescent Pollutants in Aquatic Environments. Volume 1: Oils. University of Oldenburg, Germany.

Hengstermann, T., and Reuter, R., 1992c, Laser remote sensing of pollution of the sea: a quantitative approach. EARSeL Advances in Remote Sensing, 1, 52-60.

Hoge, F.E. and Swift, R.N., 1980, Oil film thickness measurement using airborne laser-induced water Raman backscatter. Applied Optics, 19, 3269-3281.

Hoge, F.E. and Swift, R.N., 1983, Experimental feasibility of the airborne measurement of absolute oil fluorescence spectral conversion efficiency. Applied Optics, 22, 37-46.

Hoge, F.E., Berry, R.E., and Swift, R.N., 1986a, Active-passive airborne ocean color measurement. 1: Instrumentation. Applied Optics, 25, 39-47.

Hoge, F.E., Swift, R.N., and Yungel, J.K., 1986b, Active-passive airborne ocean color measurement. 2: Applications. Applied Optics, 25, 48-57.

Measures, R.M., 1984, Laser Remote Sensing. Fundamentals and Applications. John Wiley & Sons, New York, 510 pp.

O'Neil, R.A., Buja-Bijunas, L., and Rayner; D.M., 1980, Field performance of a laser fluorosensor for the detection of oil spills. Applied Optics, 19, 863-870.

Poole, L.R., and Esaias, W.E., 1982, Water Raman normalization of airborne laser fluorosensor measurements: a computer model study. Applied Optics, 21, 3756-3761.

Reuter, R., Diebel, D., and Hengstermann, T., 1993, Oceanographic laser remote sensing: measurement of hydrographic parameters in the German Bight and in the Northern Adriatic Sea. International Journal of Remote Sensing, 14, 823-484.

Schroh, K., and Bustorff, U.H, 1989, Monitoring of operational discharges in the Federal Republic of Germany. In: The Remote Sensing of Oil Slicks, A:E. Lodge (editor), pp. 77-86. (Chichester: John Wiley & Sons), 165 pp.

Verdebout, J., and Koechler, C., 1992, Nanosecond time resolution: technical, implementation and usefulness. EARSeL Advances in Remote Sensing, 2, 61-71.